Australian Government
Department of Defence
Defence Science and
Technology Organisation

DSTO

Flow Over a Body of Revolution in a Steady Turn

P. A. Gregory, P. N. Joubert
and M. S. Chong

DSTO-TR-1591

Australian Government
Department of Defence
Defence Science and
Technology Organisation

Flow Over a Body of Revolution in a Steady Turn

P. A. Gregory, P. N. Joubert and M. S. Chong

Maritime Platforms Division
Platforms Sciences Laboratory

DSTO–TR–1591

ABSTRACT

While the mechanisms of flow separation for a submarine in steady rectilinear flow are well understood, the flow separation behaviour of a submarine during a manoeuvre is not as well understood. The importance of this has led us to investigating the flow separation over a submarine-like body of revolution in a turn of fixed radius.

The flow separation over the manoeuvring body is examined by using a deformed body placed in rectilinear flow to simulate the flowfield created by a body moving through a circular path. This method was used by Von Karman at the Guggenheim Airship Laboratory and by Gurzhienko in Moscow in the 1930s to investigate the manoeuvring of airships.

The deformed model is constructed such that the local angle of attack is the same for a regular model placed in curved streamlines. Velocity should be varied linearly across the test section to ensure the local velocities at the deformed model surface are equal to the velocity along the manoeuvring model.

Numerical simulations conducted using the CFD code FLUENT show the validity of this transformation. Results for a body placed in a rotating reference frame are compared to a deformed body in rectilinear flow.

Published by

DSTO Platforms Sciences Laboratory
506 Lorimer St,
Fishermans Bend, Victoria, Australia 3207

Telephone: *(03) 9626 7000*
Facsimile: *(03) 9626 7999*

AR No. 013-126
October, 2004

APPROVED FOR PUBLIC RELEASE

Flow Over a Body of Revolution in a Steady Turn

EXECUTIVE SUMMARY

The problem of obtaining detailed data of the flow over a body of revolution in a steady turn is approached in an innovative way. A co-ordinate transformation is applied to produce a curved model which, when placed in a steady rectilinear flow, re-creates the flow geometry of a straight body in curved flow. Since the curved model is sitting in a steady flow situation (which can be created with a wind or water tunnel) detailed flow measurements of the vortices created by turning objects can be performed.

In this report, an analysis of the co-ordinate transformation is presented. Preliminary numerical studies have been conducted with the CFD code FLUENT. A body of revolution was placed in a rotating reference frame to simulate the flow over this body in a gentle turn. The results of this simulation were compared to the corresponding curved body (whose geometry is related to the turn radius and angle of attack of the turning body) in rectilinear flow. Results were obtained for both the surface flow features (such as average static pressure and skin friction distributions) and downstream flow features (the formation of the main off-body vortex).

The results show that the distributions of skin friction along the curved and straight models differ slightly, in that we observe more flow separation for our curved bodies. This gives a correspondingly lower average pressure for the curved body. In addition, the strength of the vortex produced by the curved body is lower. Further numerical work will investigate the effects of the coriolis and centrifugal forces on the formation of the off-body vortex.

These results show at this stage that any experiments incorporating this method of curved bodies will be able to replicate the dominant flow features that occur over a straight body performing a steady turn.

Authors

Paul A Gregory
Maritime Platforms Division

Paul Gregory joined the Airframes and Engines Division in 1998 after graduating from the University of Melbourne with combined degrees in mechanical engineering and science. While at AED, he worked on the prediction of Infra-Red Signatures.

He transferred to Maritime Platforms Division in 2000 where he was appointed as a Cadet Research Scientist. He is currently studying his Ph.D. at Melbourne University with support from the Maritime Platforms Division.

Professor Peter N Joubert
University of Melbourne

Professer Peter Joubert is Emeritus Professor of Mechanical Engineering at the University of Melbourne, where he has been working since 1953. He has made substantial contributions to Fluid Mechanics through his long record of research into the mechanics of flow in turbulent boundary layers. He has made many original contributions to the science and art of the prediction of boundary layer development and the fundamental frictional effects it gives rise to. He has advised the Australian government in relation to the flow and noise problems experienced by the Collins class submarines. His recent research includes the use of rotating wind tunnels to invesitgate the effect of rotation on boundary layer motion, and the innovative use of curved models to investigated separated flow over submarine hulls when manoeuvring.

Professor Min Chong
University of Melbourne

Professor Chong's research is in fluid mechanics, particularly in the study of eddying motions and turbulence. His earlier work was on the use of flying hot-wires to obtain phase-averaged velocity vector fields, and the development of critical point theory to study the topology of flow patterns. A novel technique, based on invariants of the velocity gradient tensor, was later developed to study the fine scale motions. The focus of his current research is on scaling laws in high Reynolds number turbulence. The correct form of these scaling laws is crucial, as the aerodynamic design of aircraft, ships and submarines depends on accurate knowledge of such scaling laws.

Contents

Appendices

Figures

Tables

Glossary

AVD Air Vehicles Division

MPD Maritime Platforms Division

CFD Computational Fluid Dynamics

κ Turbulent kinetic energy

ϵ Turbulent dissipation rate

y^+ Wall-normal distance normalised by friction velocity and kinematic viscosity

Re_y Reynolds number based on wall-normal distance

1 Overview and Literature Survey

1.1 Introduction

The behaviour of a fluid flowing over a body in a manoeuvre is a problem that is present in many fields of research.

Most of the research into the flow fields created by a manoeuvring object has been related to the calculation of dynamic stability derivatives. These derivatives are required during the design process and performance evaluation of any object designed to execute a controlled manoeuvre in a fluid, be they aeronautical in nature (aircraft, missiles, ballistic shells) or maritime (ships, submarines, torpedoes). When the object in question is considered to execute a turn with a fixed radius, the results can be applied to fields such as turbomachinery and wind-turbines.

A greater understanding of unsteady fluid flow in recent years has focused research into the forces on the structure of the body caused by unsteady fluid flow. In particular, studies of vortex breakdown have been carried out to investigate the induced vibration of aircraft control surfaces.

Unsteady flow becomes a major problem for maritime craft as it can induce vibrations of the propeller, caused by the sudden changes in the effective angle of incidence of the propeller blades as they rotate through the unsteady flow. Vortices themselves create excessive hydro-acoustic noise. In the specific case of a submarine's acoustic signature, it is of great importance to minimise and preferably eliminate any flow separation in order to reduce the hydro-acoustic noise from the overall acoustic signature. While the mechanisms of flow separation are well understood for a submarine in steady flow, the flow separation behaviour (and hence the changes in the hydro-acoustic signature) of a submarine during a manoeuvre are not as well understood.

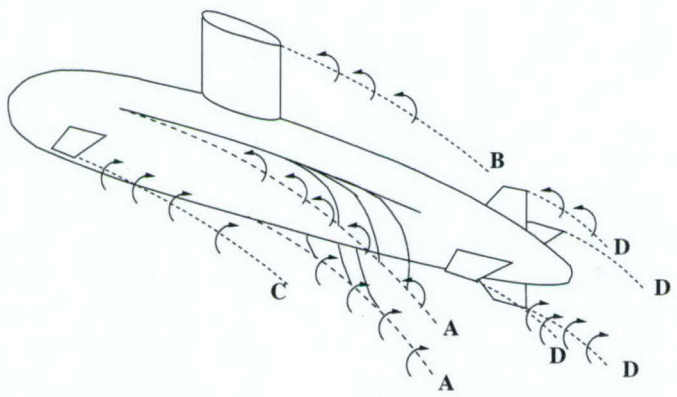

Figure 1: System of vortices produced by a submarine in a manoeuvre (taken from Lloyd and Campbell)

Figure 1 shows the system of vortices produced by a submarine during a turn. Each appendage on a submarine will produce its own system of vortices, such as the sail (B), tailplane (C) and rudder and tail-fins (D). The strength of these vortices is far less than

those cast off the body itself (A). These two vortices are produced by the cross-flow separation over the body of revolution. As the angle of attack increases along the body (see figure 4), the fluid flows over the outboard side of the body to the inboard side. At this point, the flow is no longer aligned with the body of revolution, but is in fact flowing across the circular hull cross-sections. At some point along the body, this flow will start to separate, and an off-body vortex is produced.

1.2 Analysis of a rudder-induced manoeuvre

Lewis [1] provided an extensive review of controllability and model testing in relation to issues of Naval Architecture. Chapter Nine of this volume, compiled by C.L. Crane, H. Eda and A. Landsburg contains a detailed study of the analysis of a ship in a turn.

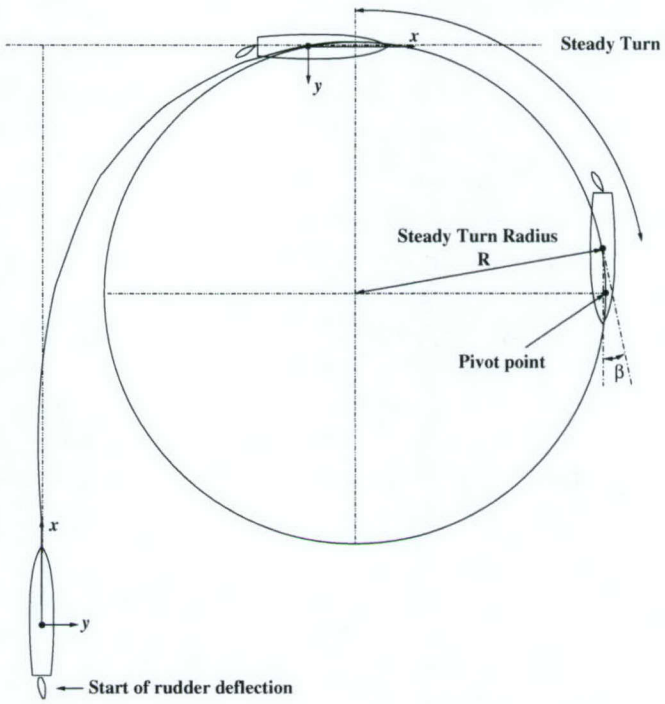

Figure 2: Path of an object in a rudder-induced turn (taken from Lewis)

Consider a ship moving through the water in a straight path with a steady velocity (figure 2). The ship experiences forces only along its x-axis. The thrust force produced by the propeller is balanced by the viscous drag forces acting on the hull and its appendages. When the rudder is deflected, it produces a force which has a component along the y-axis of the ship. For a starboard turn, the rudder is deflected towards starboard, producing a force in the port direction, pointing away from the centre of turn. This force produces a moment that causes the ship to rotate about its z-axis. The stern of the ship will move to port, while the bow of the ship will rotate towards the centre of the turn. This rotation causes the bow of the ship to point into the turn with a positive angle of attack, or drift angle β. The hydrodynamic forces acting on the ship's hull which is placed at a positive angle β to the flow will produce a force which is directed towards the centre of turn. This

force will create a change in the lateral movement of the center of gravity. In general, as the drift angle β increases, the hydrodynamic force acting on the hull towards the turn centre will increase as well. Therefore, in order to perform a tighter turn, the drift angle must be large.

When the rudder remains in a fixed position, a steady turn will develop. In this situation, the hydrodynamic and inertial forces and moments are balanced, and the path of the centre of gravity is a circular arc.

The immediate response of a ship to the deflection of the rudder produces a transient turning profile where large surge, sway and yaw accelerations occur. Since this project is concerned with the fluid flow over a body in a steady turn, the initial transient behaviour will not be considered.

The location of the *pivot point* in a steady turn locates the position on a ship where the flow of water past the ship is parallel to the ship's x-axis. The location between the pivot point and the centre of gravity can be given by $x_c = Rsin\beta$, where R is the turn radius. Since small radius turns are usually associated with large drift angles, and large radius turns with small drift angles, the product $Rsin\beta$ does not vary significantly for different ships, or indeed the same ship performing turns of different radius. For most ships the pivot point lies between the bow and 1/5 aft of the bow (see Mandel [2]). Based on empirical data, the drift angle β can be computed either as:

$$\beta = 22.5L/R + 1.45 \tag{1}$$

or

$$\beta = 18L/R \tag{2}$$

Using equation 1 gives values of x_c ranging from 0.4 to $0.5L$. Equation 2 gives $x_c = 0.3L$.

Once the ship has settled into the steady part of the turn, the accelerations in the radial direction $\dot{r}$ and along the y-axis $\dot{v}$ are zero. The linearised equations of motions for a steady turn can be written as :

$$-Y_v v - (Y_r - \Delta u_1) = Y_\delta \delta_R \tag{3}$$

$$-N_v v - N_r r = N_\delta \delta_R \tag{4}$$

where :

Y = force along the y axis of the ship (sway)

N = moment about the z axis of the ship (yaw)

v = velocity along the y axis of the ship

r = rate of rotation about the z axis of the ship

u_1 = initial equilibrium value of x-component velocity

$Y_r = \frac{\partial Y}{\partial r}$

$Y_v = \frac{\partial Y}{\partial v}$

$N_r = \frac{\partial N}{\partial r}$

$N_v = \frac{\partial N}{\partial v}$

Δ = mass

δ_R = rudder deflection angle

If the stability derivatives Y_r, Y_v, N_r, N_v and control derivatives Y_δ and N_δ are known, then equations 3 and 4 can be solved for r and v. The solutions show that the steady turning radius is proportional to ship length and inversely proportional to δ_R, and that β is directly proportional to δ_R. This linear analysis is useful for estimating steady turning radii and β for large diameter turns, but for ships in a tighter turn, the validity of the linear equations of motion breaks down.

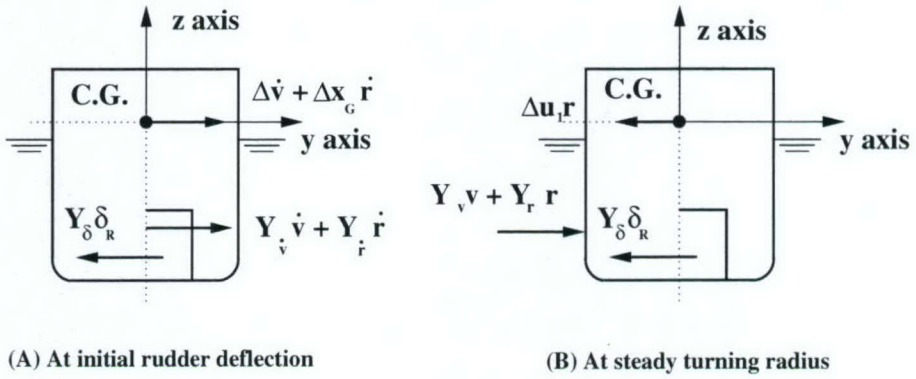

Figure 3: Location of forces for a ship in a starboard turn looking aft (taken from Lewis)

The use of a rudder also introduces pitching and rolling motion (see figure 3). Note that part(B) of figure 3 is a graphical representation of equation 3. The rolling motion in a steady turn is created by the moment caused by the rudder force ($Y_\delta \delta_R$) which points away from the turn centre, and the force on the hull ($Y_v v + Y_r r$) acting towards the direction of turn. A ship will tend to have outboard roll angle during a steady turn (i.e. lean away from the turn), whereas a submerged submarine will always lean into the turn. This is due to the location of the line of the hull force $Y_v v + Y_r r$, which because of the presence of the sail is considerably higher relative to the centre of gravity than for a surface ship. The sail on a submarine acts as a lifting device during a steady turn, so the sail contributes to the magnitude and height of the $Y_v v$ force which increases the rolling moment. Due to this increase of $Y_v v$ force a submerged turning submarine will initially experience a large inboard roll called a *snap roll*, followed by smaller inboard rolls. Arentzen and Mandel [3] investigated the importance of the sail configuration in the amount of roll induced in a turning manoeuvre, concluding that the presence of a sail increases the roll excitation in a turn, but also increases the magnitude of roll damping, and therefore dampens the amplitude of the overshoot of the snap roll.

1.3 Manoeuvring characteristics of bodies of revolution

There exists a large body of work in the open literature regarding the nonlinear aerodynamic performance of bodies of revolution. In particular this work has been approached from the area of ballistic research, and is mainly concentrated on the calculation of pitching and rolling-moment calculations for ballistic projectiles. A lot of theoretical and experimental work was conducted at NASA Ames Research Centre in the late 1960s and early 1970s (see Tobak *et. al* [4], Schiff and Tobak [5], Levy and Tobak [6]). This experimental work focused on the measurement of forces and moments for bodies of revolution at high Mach numbers. Flow-visualisation work was also performed using the vapour-screen method, revealing the dependence of some moment-coefficients on the appearance of displaced vortices. Schiff [7] used a simple numerical scheme to solve for inviscid flow of a perfect gas around a body performing both pitch and roll in supersonic flow. Schiff used a rotating co-ordinate frame to simulate the manoeuvring of the projectile. The flow was steady within the rotating frame, allowing the steady Euler equations to be solved. Good agreement was achieved with experimental data for moderate values of crossflow flight velocity. Schiff's work was carried further by Weinacht and Sturek [8] and Weinacht [9] who used the thin-layer Navier-Stokes equations to compute pitch damping coefficients for particular projectile geometries. Further work using rotating reference frames was conducted by Buckland [10] and Lesage [11]. Lesage used the commercial CFD code, TASCflow, to solve the Reynolds-averaged Navier-Stokes equations, using the $k - \epsilon$ turbulence model and wall functions to calculate the Reynolds stresses and thermal diffusion for turbulent solutions.

1.4 Manoeuvring characteristics of ships and submersibles

Extensive research has been conducted in investigating the manoeuvring characteristics of ships, and more recently, submersibles. A lot of this research has focused on the methods of ship design, and in particular methods to predict ship performance at an early design stage. Work conducted by Burcher [12,13] describes the various methods of model testing used to measure stability and control characteristics of ship forms. Burcher describes free model tests using radio controlled scale models, and constrained model tests. Constrained model tests included both rotating arm tests and oscillatory testing using a Planar Motion Mechanism. Fujino [14] examined the effects of frequency dependence on stability derivatives for ship motion.

Feldman [15] conducted rotating arm and oscillatory experiments to investigate stability and control characteristics of submarines and submersible vehicles. Mendenhall *et. al* [16] conducted a thorough investigation into the vortex shedding from circular and non-circular bodies at high angles of attack. The analytical methods he developed to predict vortex shedding were used to predict both the aerodynamic characteristics of missiles, and the hydrodynamic characteristics of submersibles in a manoeuvre (see Mendenhall and Perkins [17]).

1.5 Vorticity measurements of a manoeuvring submarine

A thorough experimental program has been conducted by Lloyd [18] and Lloyd and Campbell [19]. Lloyd proposed the use of a simple vortex-based computer program SUBSIM which would provide an early approximation of the forces and moments on a submarine hull during a manoeuvre. The aim of SUBSIM was to bridge the gap between the traditional stability derivative approach to the prediction of manoeuvring characteristics, and the use of CFD (which at that time was not mature) to estimate the forces and moments on a body.

The flow over a manoeuvring submarine is dominated by vortices which are shed from the hull and appendages (such as bow planes and the sail). The strength and position of the appendage vortices can be predicted using lifting line theory. The body vortices are affected by the angle of incidence and rate of turn of the submarine. SUBSIM was designed to use empirical formulae to represent the positions and strengths of these body vortices.

Lloyd tested three submarine-like [1] bodies of revolution in a water tunnel in both rectilinear and rotating flow. He used a probe developed by Freestone [20] to measure the strength of the vortices cast from the hull. Measurements of vorticity were taken at 10 degree angular intervals and 25 mm radial steps from the body surface. Experimental variables such as angle of incidence and turn radius were varied. By varying the angle of incidence, Lloyd was able to shift the pivot point along the model, although for the models in a tight turn, he still had large local angles of incidence at the nose. This contradicts the work of Mandel [2] who showed that the local angle of incidence at the nose approached zero as the turn radius decreased. Lloyd's experiments showed that for a body executing a turn with a large radius, the flow approached from the outboard side of the body, and vortices were shed from the inboard side. When the body was placed in a tighter turn, and the pivot point located aft of the bow, the local flow direction at the nose was from the inboard side of the body, and over the tail sections of the hull, the flow direction was from the outboard side. Lloyd hypothesised that this would produce areas of mixed vorticity, with the vortices cast from the nose convecting along the body, and then interacting with the vortices of opposite sign which were cast from the tail. His results show some evidence of this. Lloyd concluded that the flow curvature generally increases the vortex strengths but did not noticeably shift the location of the vortices. The presence of a secondary system of vortices of opposite sense generally located on the outboard side of the body were responsible for limiting the total amount of circulation in tight turns.

Lloyd held the body in a fixed attitude while changing the turn radius. It should be noted that in a tighter turn of smaller radius, the centrifugal forces will be larger (assuming the turn rate is constant). So the inward radial body surfaces forces must increase to oppose the increase in centrifugal force. Therefore the drift angle must increase, causing the radial component of the propeller thrust to increase along with the radial component of the surface pressure forces. So the location of the pivot point will move closer to the nose of the body.

Wetzel *et. al* [21] examined the crossflow separation of flow over a submarine in a turning manoeuvre, and investigated the effects of vortex generating fins and jets on the

[1] i.e with rounded noses, pointed tails and a long parallel mid-sections

location of this separation line. Wetzel was limited to placing the submarine model in a yawed position in rectilinear flow. He observed changes in the forces and moments on the model due the the delayed separation of the vortex when using fins. This experimental configuration was able to produce a flow-field which simulated a body in a gentle turn, but simply yawing a body is unable to produce the variation in angle of incidence along the hull section that is present when an object is performing a tighter turn.

1.6 Numerical simulation of a manoeuvring submarine

In recent years, the availability of large computational resources and developments in turbulence modelling has resulted in several numerical studies of flow over a submarine model (see Kempa *et. al* [22], Feng *et. al* [23], Taylor *et. al* [24]). The latest efforts of Pankajakshan *et. al* [25], continuing the work of Taylor *et. al* [24] have resulted in the ability to simulate rudder-induced manoeuvres of a submarine model with a rotating propulsor, by combining an unsteady Reynolds-averaged Navier-Stokes equations solver with a six degree of freedom rigid body model. Their solutions contain a number of interesting features, including :

1. The use of a multiblock dynamic grid system.
2. The use of deformable grid to simulate control surface movement.
3. Incorporation of both the $k - \epsilon$ and $k - \omega$ turbulence models on the hull geometry.
4. The use of a body force propulsor model and a rotating blade propulsor using the $k - \omega$ turbulence model.

1.7 The use of deformed models

At the outset of this project, Professor Peter Joubert suggested a novel experimental method which simulates the flow curvature that is created when a body is executing a steady turn of constant radius. The experimental model is itself bent around the radius of turn and placed in a straight (rectilinear) flow. In this way, the variation of the angle of attack (α), along the length of the model is the same as for a turned model. The advantages of this method include :

1. There is no requirement for complicated and expensive rotating machinery.
2. The object does not rotate, hence it cannot pass through its own wake (as can occur with rotating-arm experiments).
3. It is far easier to observe the flow field and to record detailed measurements from a stationary model than from a rotating one.
4. There is no time limit to record measurements, unlike a rotating arm which is limited to one revolution before it passes through its own wake.

Since then, a literature survey conducted by the authors has shown that this method has been used previously to determine rotational derivatives for aircraft, and to study flow curvature effects on wind-turbine blades.

As far as the authors can ascertain, the first recorded use of this method was carried out at the EAO TsAGI in Moscow in the 1930's. It was financed by the NIO Dirigiblestroy (Airship industry) to investigate the stability derivatives of airships. The work was first suggested by Prof. Vetchinkin, who in turn refers to some early theoretical work conducted by Glauert in estimating the effect of wing rotation on lift. A thorough analysis was carried out by Gurzienko [26] in 1934. It is also known that Von Karman[2] used this method to carry out experiments on airships for the U.S. Navy at the Guggenheim Airship Laboratory in Akron from 1936. This method was initially applied to airships due to the importance of the calculation of stability coefficients C_{m_q} and $C_{m_{\dot{\alpha}}}$ - i.e. the derivative of pitching moment (normalised) with respect to rate of pitch (q) and rate of change of incidence ($\dot{\alpha}$). The small size of airship control surfaces means that the airship design must be inherently stable with respect to pitching, otherwise the airship may enter a pitching oscillation mode that it is unable to correct. Using this method of deformed models, these coefficients are easily obtained. More work was done in Canada during the 1950's by Foster and Haynes [27] and Rückemann [28,29] using these methods for wind tunnel testing of dynamic derivatives. As the use of more sophisticated wind-tunnel apparatus (such as dynamically oscillating the wind-tunnel models) were developed, these derivatives could be obtained without the use of curved models. The method became less widely used, although it was briefly used to calculate derivatives of ballistics in Australia by Forsyth [30].

A similar approach to the problem of flow curvature effects was conducted by Migliore *et. al* [31], Migliore and Wolfe [32]. Migliore investigated flow curvature effects on Darrieus wind turbines, a special type of turbine which has a continuous looped airfoil section that rotates around its vertical axis. If the blade chord of the airfoil section is large relative to the radius of rotation, then flow curvature effects will be significant. He then used a conformal transformation to transform the geometric airfoil in curved flow to an equivalent virtual airfoil in rectilinear flow. This transformation introduces a virtual camber and incidence into the airfoil, which enabled an investigator to compare airfoil data collected from rectilinear flow experiments and apply them to the rotating flow situation. The use of this transformation also allowed an investigator to change the surface profile of an existing airfoil section into a airfoil section that will retain the same lift and drag properties in the rotating flow of the wind turbine blade. Migliore's methods were also examined by Hirsch and Mandal [33] and Cardona [34].

2 Transforming Equations

Consider a body performing a turn around radius R_0, aligned at an angle of attack β_0 to the flow (see figure 4). From triangle BOC we find :

$$\overline{OB} = R_0 \cos \beta_0 \tag{5}$$

[2]The exact reference has yet to be found

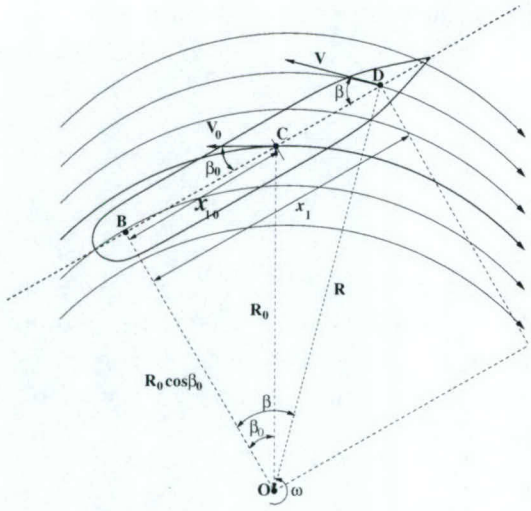

Figure 4: Body of revolution turning about point O. (not to scale)

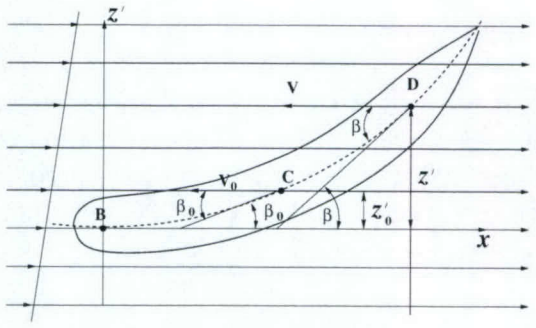

Figure 5: Body of revolution deformed about curved axis. Note the linear distribution of free-stream velocity (deformation exaggerated for clarity)

At some point D along the axis of the body, we can define the local angle of attack β as :

$$\tan\beta = \frac{\overline{BD}}{R_0 \cos\beta_0} = \frac{x_1}{R_0 \cos\beta_0} \tag{6}$$

The model axis is deformed such that the local angles of attack are preserved for rectilinear flow (figure 5) in co-ordinate system (x, z'). In this co-ordinate system :

$$\tan\beta = \frac{dz'}{dx} = \frac{x_1}{R_0 \cos\beta_0} \tag{7}$$

The length of the model axis x_1 has to be preserved. Gurzhienko[26] solved the equation for the curved model axis by computing the length of $x_1 = \overline{BD}$ using :

$$x_1 = \overline{BD} = \int_0^x \sqrt{1 + \left(\frac{dz'}{dx}\right)^2}\, dx \tag{8}$$

Combining equation 8 into equation 7, then rearranging and differentiating gives :

$$\frac{d^2 z'}{dx^2} = \frac{1}{R_0 \cos\beta_0} \sqrt{1 + \left(\frac{dz'}{dx}\right)^2} \tag{9}$$

By using reduction of order, this can be solved as a first-order linear differential equation, giving the result :

$$z' = R_0 \cos\beta_0 \left[\cosh\left(\frac{x}{R_0 \cos\beta_0}\right) - 1\right] \tag{10}$$

which describes the curvature of the centreline of the deformed model.

Independent analysis conducted by Mattner [35] at Melbourne University agrees with Gurzhienko's methods.

Gurzhienko also derived the equations which define the deformed cross-sections passing through point D as :

$$z' = x_1 \left[\cosh \left(\frac{x - x_D}{x_1} - \text{arcsinh} \frac{1}{n x_1} \right) \right] - \frac{1}{n} \tag{11}$$

where $n = R_o cos\beta_0$.

It can be shown that by deforming our body using equations 10 and 11, the change in the local angle of attack along our deformed body is usually within 2-2.5% of our original body, despite the degree of contraction and expansion along the inner and outer surfaces of the deformed model. The differences between the curved centreline and a circular arc segment is within 2% for values of $\beta_0 < 10$ degrees.

2.1 Model construction

In order to simplify model construction, it can be assumed that the cross-sections remain planar and perpendicular to the curved axis. Gurzhienko showed that for a typical model, the radius of curvature of cross sections with large diameters was typically 20 times the length of the model. The advantage of preserving the circular cross sections is that it makes fabrication of wind and water tunnel models far easier. In addition, creation of the deformed surface is also easier for use in numerical simulations.

3 Numerical Simulations

The CFD code FLUENT was used to perform simulations of flow over a body in a turn of constant radius. This was compared to rectilinear flow over the corresponding deformed body. In order to simulate the manoeuvring body, the entire flow domain was rotated around a given turn radius. In this way, the variation of magnitude and angle of attack of velocity along the body could be replicated. This does introduce a radial pressure gradient that is not present in the real situation.

3.1 Meshing scheme

The surface of the body was de-composed into logical squares so that hexahedral meshes could be used along the surface. A mapping scheme was then used to resolve the boundary layer and a volume within half the diameter of the model. Beyond this point, an unstructured tetrahedral mesh was used to fill the flow domain.

Since the boundary-layer was to be integrated all the way to wall, dense mesh spacing was required at the body surface. Several grids were generated with different wall resolutions, as well as difference flow domain sizes to ensure grid-independence.

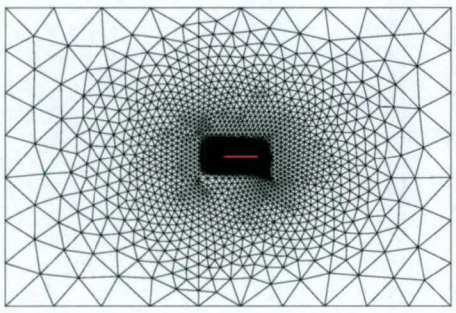

Figure 6: Detail of far-field grid

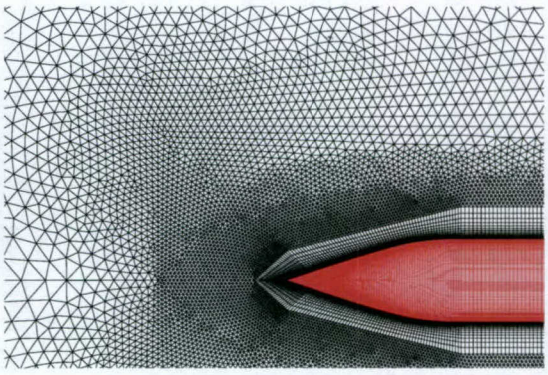

Figure 7: Detail of near-field grid

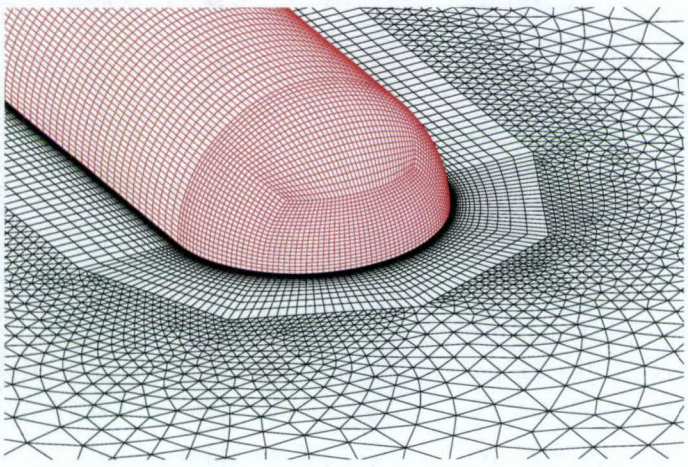

Figure 8: Detail of surface grid and boundary-layer region

3.2 Numerical scheme

Results were obtained using the Realisable $k - \epsilon$ turbulence model. The two-layer zonal method was used for wall-treatment, which requires that the first grid point in the boundary layer to be in the viscous sub-layer, i.e with $y^+ < 5$, and with at least 10 points within $Re_y < 200$. Pressure and momentum were solved using the segregated solver, with second order accuracy.

4 Results

Results have so far been obtained for a body performing a turn about a single radius. In this turn, the radius was three times the body length, with $\beta_0 = 10.5$ degrees, and the pivot point (point where $\beta = 0$) was located at the bow of the model. Further experiments will examine the effects of changes in radius, β_0 and the location of the pivot point.

Comparisons were made in the rectilinear flow cases for the curved model between simulations with a uniform freestream velocity, and those with a shear flow, where the

velocity gradient is equal to :

$$v = \omega R \tag{12}$$

where ω is the angular velocity of the model, and R is the turn radius (see figure 5). This can be transformed into the rectilinear co-ordinate system, giving :

$$v = v_o \left(1 + \frac{z'}{R}\right) \tag{13}$$

For $Re = 7.8 \times 10^6$, the average static pressure over the model is :

Average static pressure (pa)		
Co – ord. system	R_0	*Pressure*
Rotating	3L	-43.6
Rectilinear	3L	-42.8
Rectilinear (with shear)	3L	-55.5

Table 1: Average gauge static pressure on the body.

4.1 Surface features

Contour plots of wall shear stress presented in figure 9 along the rear of the body seem to indicate that the region of possible flow separation (zero wall shear stress) is larger for the curved model.

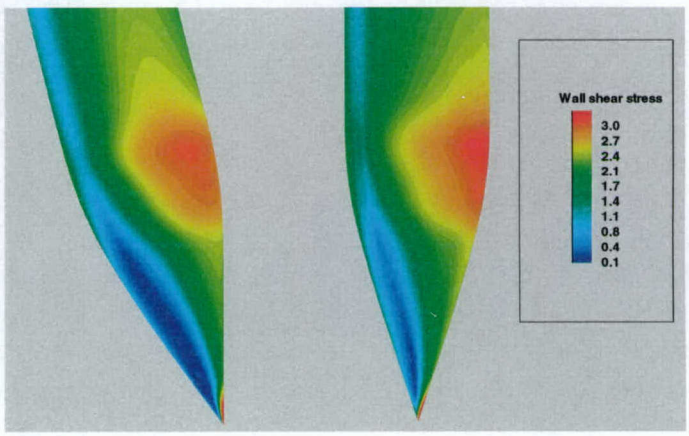

Figure 9: Detail of wall shear stress for model in rectilinear flow (left) and rotating flow (right)

Plots of path lines along the body show that flow along the separation line of the curved body leaves the surface and creates a vortex sheet (see figure 10). The same plot for the straight body in curved flow (figure 11) shows similar surface patterns, but no visible detached vortex sheet is observed. Varying the velocity magnitude along the curved body using equation 13 produced no discernible changes in the wall shear-stress and surface flow patterns when compared to the uniform flow case, although flow separation occured further upstream along the separation line.

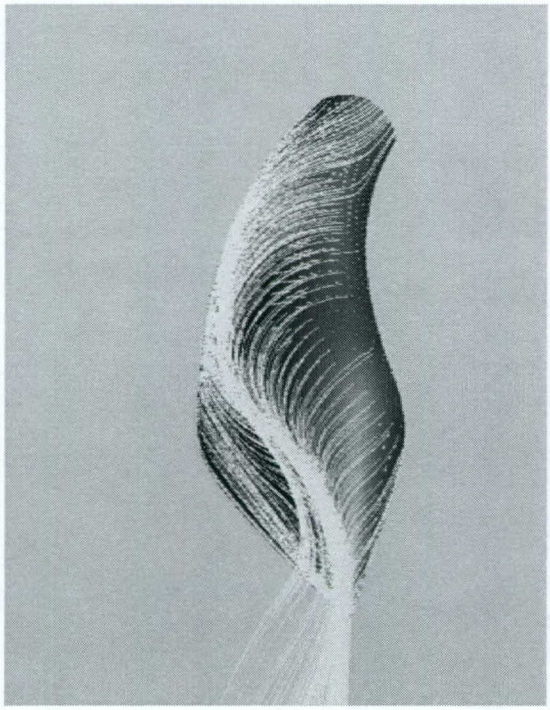

Figure 10: Pathlines of particles released from curved body surface in straight flow

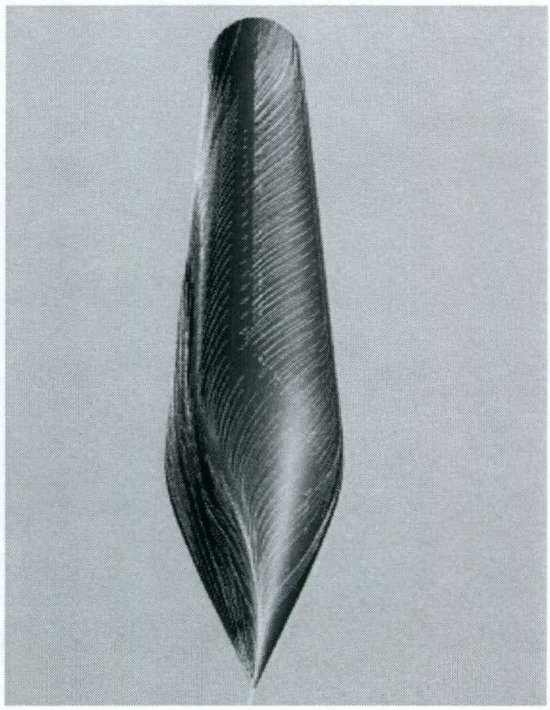

Figure 11: Pathlines of particles released from straight body surface in curved flow

4.2 Flow features

Contour plots of x-vorticity in figures 12, 13, 14 and 15 show the formation of the body vortex along the length of the models for the straight body (left), curved body (middle) and the curved body with velocity gradient (right). Regions of higher vorticity are present in the vortex produced by the straight body in curved flow. Introducing the velocity gradient across the curved model produces better quantitive agreement with peak vorticity values when compared to the straight model in curved flow. However, this causes a tighter vortex to form downstream (figure 14 and 15) when compared to the straight body. Flow separation and the formation of the vortex sheet leaving the surface can be seen in figure 14.

5 Discussion

The rotating reference frame was used as an approximation to the real situation of a body performing a turn of constant radius.

For an element of incompressible fluid in a rotating reference frame of constant angular velocity ω, the Navier-Stokes equation can be written in vector form as :

$$\frac{\partial \mathbf{u}}{\partial t} + \mathbf{u} \cdot \nabla \mathbf{u} + \mathbf{2}\omega \times \mathbf{u} = -\frac{\mathbf{1}}{\rho}\nabla p + \nu \nabla^2 \mathbf{u} \tag{14}$$

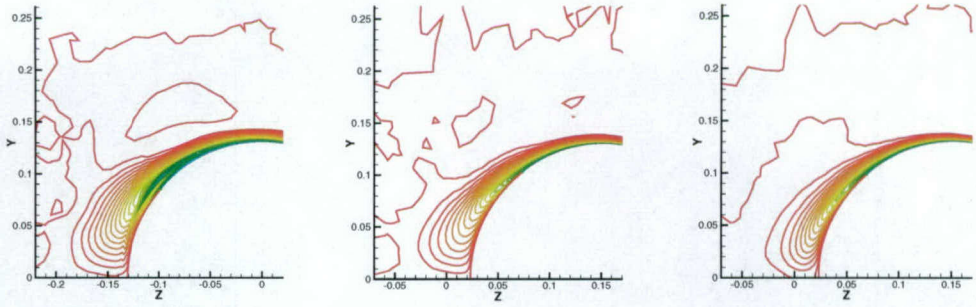

Figure 12: Contours of vorticity at $x = 0.60L$

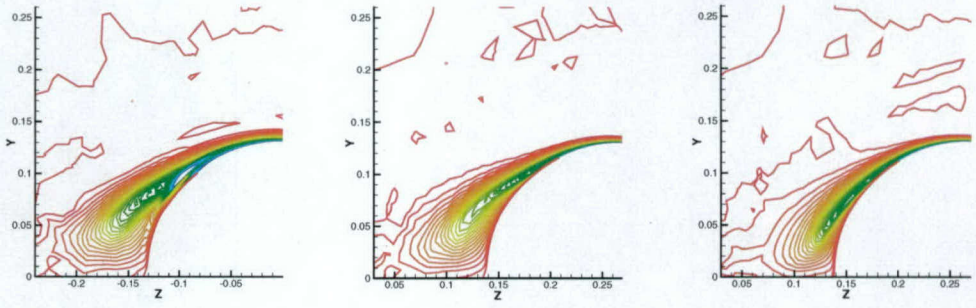

Figure 13: Contours of vorticity at $x = 0.79L$

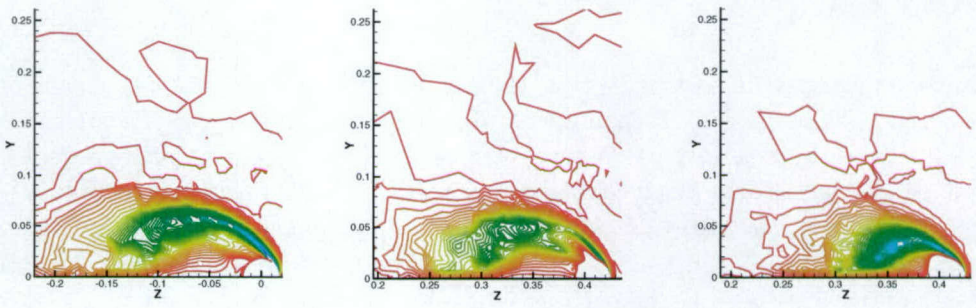

Figure 14: Contours of vorticity at $x = 0.98L$

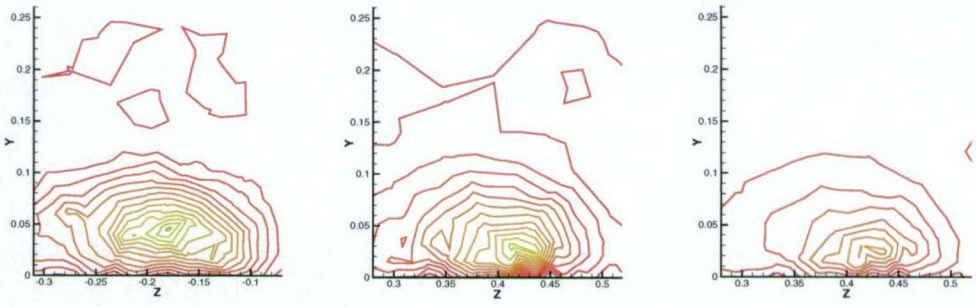

Figure 15: Contours of vorticity at $x = 1.37L$

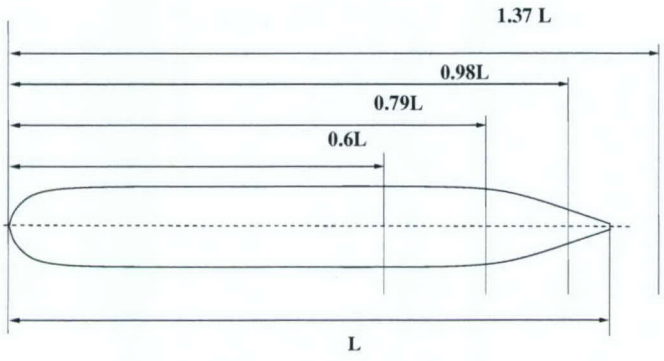

Figure 16: Location of vorticity measurement

where $2\omega \times \mathbf{u}$ is the Coriolis force, and the centrifugal force $\omega \times (\omega \times \mathbf{r})$ is incorporated into the modified pressure p, along with gravity.

In this situation, the flow will have a pressure gradient of :

$$\frac{\partial p}{\partial r} = \rho r \omega^2 \tag{15}$$

By using our co-ordinate transformation to move from curved flow to rectilinear flow, we are changing the reference frame from a non-inertial to an inertial frame. The effects of the Coriolis and centrifugal force on the boundary-layer separation and vortex formation are removed when we make our co-ordinate transformation. The use of the curved model produces a similar vortex structure to that of a straight model in curved flow, especially when we introduce a velocity gradient across the model. However, this velocity gradient may not be able to be implemented in an experimental configuration.

The differences in flow separation behaviour between the curved model and straight model may be due to several factors. Firstly, our straight model in rotating flow experiences a radial pressure gradient that would not be present for a manoeuvring body turning through a stationary fluid. Fluid flowing from the outboard side of the model to the inboard side will experience a negative pressure gradient which will help delay boundary layer separation. Comparing a model in rotating flow to experimental data of a manoeuvring body will help to determine the effect of this pressure gradient. Secondly, the presence of Coriolis and centrifugal forces may stabilise the flow over the the tail of the body. These forces are present in our simulation of the straight model in rotating flow, and they are also present in the case of a body manoeuvring through a stationary fluid. Lastly, there may be Reynolds number effects present at full scale.

Although these forces can be introduced numerically for a simulation of straight flow over a curved body, they cannot be easily incorporated experimentally. By conducting a numerical simulation of the curved body in straight flow, and including the Coriolis and centrifugal terms, their importance in the validity of this transformation could be ascertained.

6 Conclusions

Numerical simulations were conducted comparing a body placed in curved streamlines to a curved body in rectilinear flow. In order to simulate the flow over of a body performing a turn of fixed radius, a rotating flow field was used to vary the angle of attack and local velocity along the length of the body. The curved body was deformed such that the local angles of attack were preserved. In this way, the curved body was able to replicate the flowfield of the body in the rotating fluid.

Initial CFD results show good agreement between the two situations. This suggests that the vortices created by the curved body will accurately replicate the vortices created by a body in a steady turn. Therefore, any experimental results of the vortices created from a curved model can be used with confidence. Some differences were observed in the degree of flow separation between the body in rotating flow, and the curved body. These will be the subject of further investigations.

References

1. Lewis, Edward V. (ed), *Principles of Naval Architecture*, **3**, Chapeter Nine, The Society of Naval Architects and Marine Engineers, 1989
2. Mandel., P. Some Hydrodynamic Aspects of Appendage Design, *SNAME Transactions*, **61**, 1953
3. Arentzen, E. S. and Mandel., P. Naval Architecture Aspects of Submarine Design, *SNAME Transactions*, **68**, 1953
4. Tobak, M. and Schiff., L. and Peterson, L., Aerodynamics of Bodies of Revolution in Coning Motion, *AIAA* **7**, 1969, 95–99
5. Schiff., L and Tobak, M., Results from a New Wind-Tunnel Apparatus for Studying Coning and Spinning Motions of Bodies of Revolution, *AIAA* **8**, 1970, 1953–1957
6. Levy, L. L. Jr. and Tobak, M., Nonlinear Aerodynamics of Bodies of Revolution in Free Flight,*AIAA* **8**, 1970, 2168–2171
7. Schiff, L. Nonlinear Aerodynamics of Bodies in Coning Motion, *AIAA*, **10**, 1972, 1517-1522
8. Weinacht, P and Sturek, W. B. Navier-Stokes Predictions of Pitch Damping For Finned Projectiles Using Steady Coning Motion, *AIAA 8th Applied Aerodynamics Conference*, August, 1990
9. Weinacht, P., Navier-Stokes Predictions of the Individual Components of the Pitch-Damping Coefficient Sum, *Journal of Spacecraft and Rockets*, Sep-Oct, 1998
10. Buckland., R. W. Derivation of Aerodynamic Damping Coefficients from Steady-Stade Flow Computations, *Defence Research Agency*, Farnborough, Hampshire, 1996
11. Lesage., F. Navier-Stokes Prediction of Pitch Damping Coefficients for Projectiles, *Defence Research Establishment*, Valcartier, Quebec, 1997
12. Burcher, R. K. Model Testing, *Journal Mechanical Engineering Sciences*, **14**, 1972, 62–69
13. Burcher, R. K. The Prediction of the Manoeuvring Characteristics of Vessels, *Phil. Trans. R. Soc. Lond.*, **334**, 1991, 265–279
14. Fujino, M., The Effect of Frequency Dependence of the Stability Derivatives on Maneuvering Motion, *Int. Shipbuilding*, **22**, 1979
15. Feldman, J. Straightline and Rotating Arm Captive-Model experiments to investigate the stability and control characteristics of submarines and other submerged vehicles, *David W. Taylor Naval Ship Research and Development Center*, November, 1987
16. Mendenhall, M. R. and Spangler, S. B. and Perkins, S. C. Jr., Vortex Shedding from Circular and Noncircular Bodies at High Angles of Attack, *17th Aerospace Sciences Meeting*, January, 1979

17. Mendenhall, M. R. and Perkins, S. C. Jr., Prediction of the Unsteady Hydrodynamic Characteristics of Submersible Vehicles, *4th International Conference on Numerical Ship Hydrodynamics*, September, 1985

18. Lloyd, A. R. J., Progress Towards a Rational Method of Predicting Submarine Manoeuvres, *RINA Symposium on Naval Submarines*, May, 1983, London

19. Lloyd, A. R. J. and Campbell I. M. C., Experiments to Investigate the Vortices Shed from a Submarine-Like Body of Revolution, *59th meeting of the AGARD Fluid Dynamics Symposium*, 1986

20. Freestone, M. M., Vorticity Measurement by a pressure probe, *Aeronautical Journal*, January, 1988, 29–35

21. Wetzel., T. G. and Simpson, R. L. and Liapis, S., The Effects of Vortex Generating Fins and Jets on the Crossflow Seperation of a Submarine in a Turning Maneuver, *Virginia Polytechnic Institute and State University*, Blacksburg, Virginia, 1993

22. Kempa, S. N. and Strickland, J. H., Hydrodynamics of Maneuvering Bodies : LDRD Final Report, *Sandia National Laboratories*, Albuquerque, New Mexico, 1994

23. Feng, Z., Numerical Simulation of Viscous Flow around an Appended Submarine Model, *Journal of Hydrodynamics*, **9**, 1997, 58–64

24. Taylor, L. K. and Pankajakshan, R. and Jiang, M. and Sheng, C. and Briley, W. R. and Whitfield, D. L., Large-Scale Simulations for Maneuvering Submarines and Propulsors, *AIAA 29th Plasmadynamics and Lasers Conference*, June, 1998, Albuquerque, New Mexico

25. Pankajakshan, R. and Taylor, L. K. and Jiang, M. and Remotigue, M. G. and Briley, W. R. and Whitfield, D. L., Parallel Simulations for Control-Surface Induced Submarine Manoeuvre, *AIAA, 38th Aerospace Sciences Meeting and Exhibit*, January, 2000, Reno, Nevada

26. Gurzhienko, G. A., Metod iskrivlenykh modelei primenenie ego k izucheniu krivolineinogo noleta vozdushnykh korablie (The method of Deformed Bodies and its use in the study of Curved Flights of Airships) *Trudy TsAGI*, **182**, 1934

27. Foster, D. J., and Haynes, G. W., Rotary Stability Derivatives from Distorted Models *Journal of the Royal Aeronautical Society*, **60**, 1956

28. Orlik - Rückemann, K., Methods of Measurement of Aircraft Dynamic Stability Derivatives, *National Research Council of Canada*, 1959

29. Orlik - Rückemann, K., Wind Tunnel Measurements of Dynamic Derivatives, *National Research Council of Canada*, 1963

30. Forsyth, G. F., An Introduction to Dynamic Derivatives (3) Methods of Oscillating Models in Pitch and Yaw in a 530 by 810 Millimetre Transonic Wind Tunnel, *DSTO, Aeronautical Reseach Laboratories*, Melbourne, Victoria, 1979

31. Migliore, P. G. and Wolfe., W. P. and Fanucci, J. B., Flow Curvature Effects on Darrieus Turbine Blade Aerodynamics *Journal of Engergy*, **4**, 1980, 49–55

32. Migliore, P. G. and Wolfe., J. B., Some Effects of Flow Curvature Effects on the Aerodynamics of Darrieus Wind Turbines *West Virginia University* , 1979

33. Hirsch, Ch. and Mandal, A. C., Flow Curvature Effects on Vertical Axis Darrieus Wind Turbine Having High Chord-Radius Ratio *European Wind Energy Conference*, 1979, 405–410

34. Cardona, J. L., Flow Curvature Effects and Dynamic Stall Simulated with an Aerodynamic Free-Vortex Model for VAWT *Wind Engineering*, **8**, 1984, 135–143

35. Mattner, T., Private Communications and notes.

Appendix A Formulation of Stability Derivatives

Stability characteristics of an aircraft for example can be obtained from an analysis of its equation of motion. These consist of three equations describing the motion of the aircraft's centre of gravity and three describing the motion of the aircraft around its centre of gravity. These equations of motion consist of mass or inertia terms, gravity, thrust and aerodynamic terms.

A system of these equations usually consists of three force and three moment equations. Aerodynamic forces and moments are represented by equations of motion in the form of series expansions in variables of motion and their time derivatives. The coefficients in these expansions are referred to as the Stability Derivatives.

A.1 Example of hydrodynamic stability derivatives

An equation for the sway force applied to a submarine can be written as

$$Y = m(\dot{v} - wp + ur) \tag{A1}$$

where

v sway (yaw) velocity of submarine

w heave (pitch) velocity of submarine

u longitudinal velocity of submarine

p roll rate

r yaw rate

Y is the force applied by the fluid to the submarine and includes contributions arising from hydrodynamic phenomena as well as from static stability contributions. Assuming that it can be expressed as a function of the instantaneous velocities and accelerations of the submarine in six degrees of freedom and the deflections of its control surfaces, then

$$Y = Y[u, v, w, p, q, r, \dot{u}, \dot{v}, \dot{w}, \dot{p}, \dot{q}, \dot{r}, \delta_b, \delta_s, \delta_r] \tag{A2}$$

where

δ_b bow plane angle

δ_s stern plane angle

δ_r rudder angle

Using a Taylor series expansion allows the fluid forces and moments to be given in terms of the sensitivity of each force and moment to each velocity, acceleration and control deflection. So for a submarine in a turn, the equation for Y becomes

$$Y = Y_v v + Y_p p + Y_r r + Y_{\dot{v}} \dot{v} + Y_{\dot{p}} \dot{p} + Y_{\dot{r}} \dot{r} + Y_{\delta_r} \delta_r \tag{A3}$$

in addition to non linear terms and static stability terms.

The coefficients are defined as

$$Y_v = \left(\frac{\partial Y}{\partial v}\right)_{v=0} \tag{A4}$$

Appendix B List of Stability Derivatives in aerodynamic notation

Static Longitudinal Derivatives

$C_{m\alpha}$ pitching moment due to angle of attack

$C_{L\alpha}$ lift force due to angle of attack

Static Lateral Derivatives

$C_{n\beta}$ yawing moment due to angle of sideslip

$C_{L\beta}$ rolling moment due to angle of sideslip

$C_{Y\beta}$ side force due to angle of sideslip

Dynamic Longitudinal Derivatives

$C_{m\dot{\alpha}}$ pitching moment due to vertical acceleration

C_{mq} pitching moment due to pitching

$C_{L\dot{\alpha}}$ lift force due to vertical acceleration

C_{Lq} lift force due to pitching

Dynamic Lateral Derivatives

$C_{n\dot{\beta}}$ yawing moment due to acceleration in sideslip

C_{nr} yawing moment due to yawing

C_{np} yawing moment due to rolling

$C_{L\dot{\beta}}$ rolling moment due to acceleration in sideslip

C_{lr} rolling moment due to yawing

C_{lp} rolling moment due to rolling

$C_{Y\dot{\beta}}$ side force due to acceleration in sideslip

C_{Yr} side force due to yawing

C_{Yp} side force due to rolling

In the case of oscillatory motion about a fixed axis, acceleration in translation (= rate of change of α or β) and rotational velocity are simultaneously present. This gives oscillatory derivatives such as $(C_{mq} + C_{m\dot{\alpha}})$ and $(C_{Lq} + C_{L\dot{\alpha}})$ for the case of pitching oscillation, and $(C_{nr} + C_{n\dot{\beta}})$, $(C_{lr} + C_{l\dot{\beta}})$ and $(C_{Yr} + C_{Y\dot{\beta}})$ for yawing oscillation.

The derivatives are usually made dimensionless in such a way that:

$$C_{m\alpha} = \left[\frac{\partial C_m}{\partial \alpha}\right]_{\alpha\to 0} \quad C_{Y\beta} = \left[\frac{\partial C_Y}{\partial \beta}\right]_{\beta\to 0} \quad C_{nr} = \left[\frac{\partial C_n}{\partial \frac{rb}{2V}}\right]_{r\to} \quad C_{L\dot{\alpha}} = \left[\frac{\partial C_L}{\partial \frac{\dot{\alpha}c}{2V}}\right]_{\dot{\alpha}\to 0}$$

etc. where :

$C_m = M/\overline{q}Sc$ = pitching moment coefficient

$C_L = L/\overline{q}S$ = lift force coefficient

$C_n = N/\overline{q}Sb$ = yawing moment coefficient, etc.

with

α = angle of attack

β = angle of sideslip

p = rolling velocity

q = pitching velocity

r = yawing velocity

V = air speed

$\overline{q}$ = dynamic pressure

S = reference area

c = reference length in longitudinal motion

b = reference length in lateral motion

DISTRIBUTION LIST

Flow Over a Body of Revolution in a Steady Turn

P. A. Gregory, P. N. Joubert and M. S. Chong

	Number of Copies
AUSTRALIA	
DEFENCE ORGANISATION	
Task Sponsor	
CANSG, CapDev, Fleet Base West, HMAS Sterling, WA	1
S&T Program	
Chief Defence Scientist FAS Science Policy AS Science Corporate Management Director General Science Policy Development	1
Counsellor, Defence Science, London	Doc Data Sheet
Counsellor, Defence Science, Washington	Doc Data Sheet
Scientific Adviser to MRDC, Thailand	Doc Data Sheet
Scientific Adviser Joint	1
Navy Scientific Adviser	1
Scientific Adviser, Army	Doc Data Sheet and Dist List
Air Force Scientific Adviser	Doc Data Sheet and Dist List
Scientific Adviser to the DMO M&A	Doc Data Sheet and Dist List
Scientific Adviser to the DMO ELL	Doc Data Sheet and Dist List
Platform Sciences Laboratory	
Chief of Maritime Platforms Division	Doc Data Sheet and Dist List
Research Leader, Undersea Platforms	Doc Data Sheet and Dist List
Head Hydrodynamics Group	4
	1 (pdf format)
Paul Gregory	3
DSTO Library and Archives	
Library, Fishermans Bend	Doc Data Sheet
Library, Edinburgh	1
Australian Archives	1

Capability Systems Division	
Director General Maritime Development	1
Director General Information Capability Development	Doc Data Sheet
Office of the Chief Information Officer	
Deputy Chief Information Officer	Doc Data Sheet
Director General Information Policy and Plans	Doc Data Sheet
AS Information Structures and Futures	Doc Data Sheet
AS Information Architecture and Management	Doc Data Sheet
Director General Australian Defence Simulation Office	Doc Data Sheet
Strategy Group	
Director General Military Strategy	Doc Data Sheet
Director General Preparedness	Doc Data Sheet
HQAST	
SO (Science) ASJIC	Doc Data Sheet
Navy	
SO (SCIENCE), COMAUSNAVSURFGRP, NSW	Doc Data Sheet and Dist List
Air Force	
SO (SCIENCE), Headquarters Air Combat Group, RAAF Base Williamtown	Doc Data Sheet and Exec Summ
Army	
ABCA National Standardisation Officer, Land Warfare Development Sector, Puckapunyal	Doc Data Sheet (emailed)
SO (Science), Deployable Joint Force Headquarters (DJFHQ)(L), Enoggera QLD	Doc Data Sheet
SO (Science), Land Headquarters (LHQ), Victoria Barracks, NSW	Doc Data Sheet and Exec Summ
Intelligence Program	
DGSTA, Defence Intelligence Organisation	1
Manager, Information Centre, Defence Intelligence Organisation	1
	1 (pdf format)
Assistant Secretary Corporate, Defence Imagery and Geospatial Organisation	Doc Data Sheet
Defence Materiel Organisation	
Head Aerospace Systems Division	Doc Data Sheet
Head Maritime Systems Division	Doc Data Sheet
Chief Joint Logistics Command	Doc Data Sheet

Management Information Systems Division	Doc Data Sheet
Head Materiel Finance	Doc Data Sheet
Defence Libraries	
Library Manager, DLS-Canberra	1
Library Manager, DLS-Sydney West	Doc Data Sheet

OTHER ORGANISATIONS

National Library of Australia	1
NASA (Canberra)	1

UNIVERSITIES AND COLLEGES

Australian Defence Force Academy Library	1
Head of Aerospace and Mechanical Engineering, ADFA	1
Deakin University Library, Serials Section (M List), Geelong, Vic	1
Hargrave Library, Monash University	Doc Data Sheet
Librarian, Flinders University	1

OUTSIDE AUSTRALIA

INTERNATIONAL DEFENCE INFORMATION CENTRES

US Defense Technical Information Center	2
UK Defence Research Information Centre	2
Canada Defence Scientific Information Service	1
NZ Defence Information Centre	1

ABSTRACTING AND INFORMATION ORGANISATIONS

Library, Chemical Abstracts Reference Service	1
Engineering Societies Library, US	1
Materials Information, Cambridge Scientific Abstracts, US	1
Documents Librarian, The Center for Research Libraries, US	1

SPARES

DSTO Edinburgh Library	5

Total number of copies:	**38 printed 2 pdf**	40

DEFENCE SCIENCE AND TECHNOLOGY ORGANISATION DOCUMENT CONTROL DATA				1. CAVEAT/PRIVACY MARKING
2. TITLE Flow Over a Body of Revolution in a Steady Turn			3. SECURITY CLASSIFICATION Document (U) Title (U) Abstract (U)	
4. AUTHORS P. A. Gregory, P. N. Joubert and M. S. Chong			5. CORPORATE AUTHOR Platforms Sciences Laboratory 506 Lorimer St, Fishermans Bend, Victoria, Australia 3207	
6a. DSTO NUMBER DSTO–TR–1591	6b. AR NUMBER 013-126		6c. TYPE OF REPORT Technical Report	7. DOCUMENT DATE October, 2004
8. FILE NUMBER 510/207/1300	9. TASK NUMBER NAV 03/136	10. SPONSOR CANSG	11. No OF PAGES 23	12. No OF REFS 35
13. URL OF ELECTRONIC VERSION http://www.dsto.defence.gov.au/corporate/reports/DSTO–TR–1591.pdf			14. RELEASE AUTHORITY Chief, Maritime Platforms Division	

15. SECONDARY RELEASE STATEMENT OF THIS DOCUMENT

Approved For Public Release

OVERSEAS ENQUIRIES OUTSIDE STATED LIMITATIONS SHOULD BE REFERRED THROUGH DOCUMENT EXCHANGE, PO BOX 1500, EDINBURGH, SOUTH AUSTRALIA 5111

16. DELIBERATE ANNOUNCEMENT

No Limitations

17. CITATION IN OTHER DOCUMENTS

No Limitations

18. DEFTEST DESCRIPTORS

Submarines
Computational Fluid Dynamics
Turning (Maneuvering)

19. ABSTRACT

While the mechanisms of flow separation for a submarine in steady rectilinear flow are well understood, the flow separation behaviour of a submarine during a manoeuvre is not as well understood. The importance of this has led us to investigating the flow separation over a submarine-like body of revolution in a turn of fixed radius.

The flow separation over the manoeuvring body is examined by using a deformed body placed in rectilinear flow to simulate the flowfield created by a body moving through a circular path. This method was used by Von Karman at the Guggenheim Airship Laboratory and by Gurzhienko in Moscow in the 1930s to investigate the manoeuvring of airships.

The deformed model is constructed such that the local angle of attack is the same for a regular model placed in curved streamlines. Velocity should be varied linearly across the test section to ensure the local velocities at the deformed model surface are equal to the velocity along the manoeuvring model. Numerical simulations conducted using the CFD code FLUENT show the validity of this transformation. Results for a body placed in a rotating reference frame are compared to a deformed body in rectilinear flow.

TECHNICAL REPORT DSTO-TR-1591 AR-013-126 OCTOBER 2004

Australian Government
Department of Defence
Defence Science and
Technology Organisation

PLATFORMS SCIENCES LABORATORY
506 LORIMER STREET FISHERMANS BEND VICTORIA 3207 AUSTRALIA
TELEPHONE (03) 9626 7000